Asia-Pacific Journal of Science and Technology: Volume: 31 Issue: 06 Article ID: APST-31-06-06 Research Article

APST

Asia-Pacific Journal of Science and Technology

https//:www.tci-thaijo.org/index.php/APST/index

Published by Research and Innovation Department,
Khon Kaen University, Thailand

Physiological and Agronomic Trait Responses of Khao Wong Kalasin and RD6 Rice Cultivars to Progressive PEG-Induced Osmotic Stress

Prasit Khunsanit[1*], Phichaiphusit Bubparn[1], Tanaphoom Boonmee[1], Nattapon Kan-a-roon[1], Urai Kollboon[1] and Keeravit Petjul[1]

[1] Department of Interdisciplinary Agriculture, Faculty of Agricultural Technology, Kalasin University, Kalasin, 46000, Thailand
[*]Corresponding author: prasit.kh@ksu.ac.th

Received 8 May 2026
Revised 15 September 2026
Accepted 21 September 2026

Abstract

Osmotic stress can strongly affect rice growth and physiological performance, particularly during early development. This study compared the responses of Khao Wong Kalasin sticky rice (KW) and RD6 to progressive polyethylene glycol (PEG)-induced osmotic stress at the seedling stage. Six-week-old seedlings were grown hydroponically under greenhouse conditions and exposed sequentially to 15%, 20%, and 25% PEG 6000 for 14 days, followed by 6 days of recovery in PEG-free nutrient solution. Tiller number (TN), leaf rolling score (LRS), drought score (DS), biomass accumulation, relative water content (RWC), cell membrane stability (CMS), chlorophyll content, and logistic growth parameters were evaluated. Lower values of TN, shoot and root biomass, RWC, CMS, and several chlorophyll traits were observed under progressive PEG-induced osmotic stress, whereas LRS and DS showed higher numerical values in both cultivars. KW showed greater numerical reductions in biomass and water-related traits, whereas RD6 maintained relatively higher biomass, RWC, and CMS under severe stress. Logistic analysis showed substantially lower predicted maximum biomass (Md_m) and instantaneous growth rate (dMd/dt) under progressive PEG stress, with a greater numerical reduction in Md_m in KW. Following PEG removal, responses varied among traits and cultivars, and increases in chlorophyll did not necessarily indicate complete restoration of photosynthetic function. Overall, KW and RD6 exhibited distinct physiological and agronomic trait responses to progressive PEG-induced osmotic stress at the seedling stage. Because each treatment condition was represented by a single container, comparisons between treatment conditions were interpreted descriptively rather than as inferential evidence of treatment effects.

Keywords: biomass, cell membrane stability, osmotic stress, Khao Wong Kalasin sticky rice, logistic function, relative water content, water deficit

1. Introduction

Rice cultivation in northeastern Thailand (Isan) is predominantly rainfed, with approximately 90% of production relying on rainfall [1]. Consequently, drought represents a major abiotic constraint that limits plant growth and reduces yield [2, 3]. Developing drought-tolerant rice varieties is therefore a key strategy to mitigate the adverse effects of water deficit and enhance yield stability under rainfed conditions [4]. In this context, local and wild rice varieties constitute important genetic resources, as they harbor substantial genetic diversity and adaptive traits that can be exploited in breeding programs for drought tolerance [5].

Khao Wong Kalasin sticky rice was granted Geographical Indication (GI) certification by the Department of Intellectual Property, Thailand, on 9 June 2009. The GI product is based on the traditional Khao Wong landrace (Khao Gor Deaw), a locally adapted glutinous rice variety cultivated in the Khao Wong production area. The area is characterized by a basin landscape surrounded by mountains, creating a circular topography from which the name “Khao Wong” is derived (“khao” meaning mountain and “wong” meaning circle in Thai). The region has a relatively cool and dry climate with limited water availability, which may have contributed to the adaptation of the local rice landrace to water-limited conditions [6].

In the present study, the Khao Wong landrace (KW) and RD6 were selected as contrasting glutinous rice genotypes for comparative evaluation of osmotic-stress responses. KW represents a traditional, locally adapted landrace, whereas RD6 is an improved cultivar developed from Khao Dawk Mali 105 (KDML105) through gamma-ray-induced mutation breeding. Their contrasting origins and breeding backgrounds provide a useful basis for investigating differences in physiological and agronomic trait responses to progressive osmotic stress. However, the responses of these two genotypes to progressive PEG-induced osmotic stress, particularly with respect to growth, biomass accumulation, water status, cell membrane stability, and chlorophyll traits, remain insufficiently characterized. In addition, changes in biomass accumulation dynamics under progressive osmotic stress and the extent of subsequent recovery have not been comprehensively evaluated in these two contrasting genotypes. Therefore, this study aimed to compare the physiological and agronomic trait responses of KW and RD6 to progressive PEG-induced osmotic stress and subsequent recovery. By integrating multiple physiological and agronomic traits with logistic growth analysis, this study provides a comparative characterization of cultivar-specific responses to progressive osmotic stress at the seedling stage. The findings may provide useful information for characterizing osmotic-stress responses in rice germplasm and for guiding further evaluation under soil- and field-based drought conditions.

2. Materials and Methods

2.1 Plant material and growth conditions

The experiment was conducted in a greenhouse under ambient environmental conditions, without control of temperature, relative humidity, or light intensity, at the Faculty of Agricultural Technology, Kalasin University, Thailand, from January to April 2026. The plants were exposed to the prevailing greenhouse conditions throughout the experimental period. The experiment consisted of two treatment conditions: non-stress (0% PEG) and progressive PEG-induced osmotic stress. One container was assigned to each treatment. Both KW and RD6 were grown within each container. Because only one container was used for each treatment, treatment conditions were not independently replicated. Therefore, the four plants sampled at each sampling time were treated as subsamples within the respective container rather than independent experimental replicates. All comparisons between non-stress and PEG-induced osmotic stress are therefore interpreted descriptively and should not be considered inferential evidence of treatment effects. Progressive osmotic stress was imposed by sequentially increasing the PEG 6000 concentration from 15% to 20% and then to 25%, representing progressive stress stages rather than independent treatment levels. At each sampling time, four plants of each cultivar were randomly selected from each treatment container for destructive sampling. These plants were considered subsamples within the respective container and not independent experimental replicates. Seeds were germinated in water for two weeks and subsequently transferred to a nutrient solution (AB mix) for hydroponic cultivation, following the method described by Balansag et al. (2023) [7], and grown for an additional four weeks. Seedlings were grown individually in 20-cm³ cells of a tray measuring 36 × 14 × 40 cm and were supported by hydroponic sponges. Seeds of the Khao Wong Kalasin landrace (Khao Gor Deaw) and RD6 were obtained directly from local farmers in Kalasin Province, Thailand. Before germination, seeds were visually inspected, and healthy, undamaged seeds of relatively uniform size were selected. The seeds were germinated under the same conditions before being transferred to the hydroponic system.

The nutrient solution consisted of two stock formulations. Formula A contained calcium nitrate ($Ca(NO_3)_2$; 115 g L^{-1}), Fe-EDTA (13.2% Fe; 4 g L^{-1}), Fe-EDDHA (7% Fe; 2 g L^{-1}), and boric acid (H_3BO_3; 20.5% B; 1 g L^{-1}), while formula B contained potassium nitrate (KNO_3; 100 g L^{-1}), magnesium sulfate ($MgSO_4$; 50 g L^{-1}), monopotassium phosphate (KH_2PO_4; 27 g L^{-1}), monoammonium phosphate ($NH_4H_2PO_4$; 5 g L^{-1}), Cu-EDTA (14% Cu; 1 g L^{-1}), Mn-EDTA (12% Mn; 1 g L^{-1}), Zn-EDTA (14% Zn; 1 g L^{-1}), and trace elements (Ni, Cu, Mn, Zn, Fe, B, Mo, and Mg; 5 g L^{-1}). Stock solutions of formulas A and B were prepared separately by dissolving each in 5 L of water. For nutrient solution preparation, 20 mL of each stock solution was added to 10 L of water.

Groundwater (EC ≈ 0.15 dS m^{-1}) was used to prepare the nutrient solution, resulting in a final electrical conductivity (EC) of approximately 0.52 dS m^{-1}. Six-week-old seedlings grown under non-stress conditions were then subjected to osmotic stress by the stepwise addition of polyethylene glycol (PEG 6000) to the AB mix. PEG 6000 solutions were prepared on a weight/volume (w/v) basis at concentrations of 15%, 20%, and 25%. The PEG concentration was increased sequentially, with 15% PEG applied for 4 days, followed by 20% PEG for 3 days and 25% PEG for 7 days. The nutrient solution was replaced at the end of each treatment step. The non-stress control plants were maintained in PEG-free AB nutrient solution, which was replaced at the same time as that in the PEG treatments to ensure that nutrient renewal was consistent among treatments. After the stress period, plants were allowed to recover by washing the roots with distilled water to remove residual PEG and transferring them to fresh PEG-free AB nutrient solution for 6 days. No visible symptoms of nutrient deficiency were observed throughout the experimental period.

2.2 Tiller number, leaf rolling score, and drought score determination

Tiller number (TN) was determined by counting only active tillers. Leaf rolling score (LRS) was evaluated visually using a scale of 1 to 5, where 1 indicates no stress and 5 indicates dead or dying plants [8]. Drought score (DS) was assessed following De Datta et al. (1988) [9], using a scale ranging from 0 to 9, where 0 indicates no stress and 9 indicates a dead plant.

2.3 Biomass accumulation, growth analysis, and model fitting

Plants were separated into shoots and roots, and fresh mass was recorded. Samples were then dried at 70°C for 3 days or until constant weight was reached, and dry mass was determined. The shoot dry-to-fresh mass ratio (S_Md/Mf) and root-to-shoot ratio (Md_R/S) were subsequently calculated. Logistic growth analysis was performed using total dry mass (Md_t) as the response variable. Growth over time was described using a three-parameter logistic model [10, 11]:

$$Md_t = \frac{Md_0 Md_m}{Md_0 + (Md_m - Md_0)e^{-\alpha t}}$$

where Md_t represents total dry mass (g plant^{-1}) at time t (day), Md_0 is the estimated initial total dry mass, Md_m is the asymptotic maximum total dry mass, and α is the logistic rate parameter (day^{-1}) governing the temporal pattern and steepness of biomass accumulation. The term $e^{-\alpha t}$ represents the exponential component of the logistic model, where e denotes the base of the natural logarithm.

Model parameters were estimated separately for each treatment and cultivar using nonlinear least squares regression. Model fit was evaluated using the coefficient of determination (R^2) and root mean square error (RMSE), and parameter estimates were reported with their standard errors. The fitting procedure was performed in R using the *nls* function, with initial parameter values derived from observed minimum and maximum biomass. The instantaneous growth rate (dMd/dt) was calculated as the first derivative of the logistic function:

$$\frac{dMd}{dt} = \frac{Md_0 Md_m (Md_m - Md_0)\alpha e^{-\alpha t}}{[Md_0 + (Md_m - Md_0)e^{-\alpha t}]^2}$$

By setting $m = Md_m \times Md_0$ and $n = Md_m - Md_0$, the first derivative can be expressed in the following simplified form:

$$\frac{dMd}{dt} = \frac{mn\alpha e^{-\alpha t}}{(Md_0 + ne^{-\alpha t})^2}$$

Growth rates were computed across a continuous time sequence to generate smooth curves representing biomass accumulation dynamics.

2.4 Relative water content, electrical conductivity, and chlorophyll content determination

Physiological parameters were measured at the end of each stepwise PEG-induced osmotic treatment and compared with those under non-stress conditions, using four plants per cultivar at each sampling time. The youngest fully expanded leaf from the main tiller was excised and weighed to determine fresh weight. The same leaf was then destructively sampled for determination of cell membrane stability (CMS), relative water content (RWC), and chlorophyll content (Chl).

The youngest fully expanded leaf was divided into three parts for the determination of CMS, RWC, and Chl. For RWC determination, a 4-cm leaf segment was excised and weighed to obtain fresh weight (FW). The sample was then soaked in deionized water for 4 h and weighed to obtain turgid weight (TW). Subsequently, the sample was dried at 70°C for 3 days and weighed to obtain dry weight (DW). Relative water content was calculated as RWC = (FW − DW) / (TW − DW) × 100.

For CMS measurement, 15 mg of leaf tissue was weighed, cut into 0.2 cm segments, and immersed in 10 mL of deionized water (EC ≈ 0.005 dS/m) for 4 h at 25°C. Electrical conductivity (EC) was measured using a portable meter to obtain the initial conductivity (EC_0). Samples were then boiled at 100°C for 30 min, allowed to cool to room temperature, and measured again to obtain the final conductivity (EC_1). Cell membrane stability was calculated as CMS = [1 − (EC_0 / EC_1)] × 100.

Chlorophyll content was determined according to Moran (1982) [12] and expressed initially as μg mL^{-1}. The values were subsequently converted to g m^{-2} based on the leaf disc area and extraction volume. Briefly, leaf discs (0.283 cm^2) were excised and immersed in 4 mL of N,N-dimethylformamide (DMF) in amber vials without

dilution. Samples were incubated in the dark at 25°C for 5 days until complete chlorosis was observed. Chlorophyll content was measured using a spectrophotometer at 647 and 664 nm.

Chlorophyll contents (g m^{-2}) were calculated as follows:

$$Chl_a = [(-2.99 \times A647) + (12.64 \times A664)] \times Vol / (D \times Area \times 100)$$
$$Chl_b = [(23.26 \times A647) - (5.60 \times A664)] \times Vol / (D \times Area \times 100)$$
$$Chl_{total} = [(20.27 \times A647) + (7.04 \times A664)] \times Vol / (D \times Area \times 100)$$

where Vol is the extraction volume (mL), Area is the leaf area (cm^2), and D is the dilution factor (set to 1).

2.5 Percentage of reduction and recovery

Reduction, stress increase, stress severity, and recovery percentages were calculated according to the direction of each trait. For growth and physiological traits, where higher values indicate better performance, percentage reduction was calculated as [13]:

$$\text{Reduction (\%)} = 100 \times [1 - (\text{Stress} / \text{Control})]$$

For injury-related traits, such as leaf rolling score, where higher values indicate greater injury, stress increase was calculated as:

$$\text{Stress increase (\%)} = 100 \times [1 - (\text{Control} / \text{Stress})]$$

For drought score, which ranges from 0 to 9, stress severity relative to the maximum possible score was calculated as:

$$\text{Stress severity (\%)} = \text{Stress} / 9 \times 100$$

Recovery was expressed relative to the corresponding non-stress control value as [14]:

$$\text{Recovery relative to control (\%)} = \text{Recovery} / \text{Control} \times 100$$

For leaf rolling score and drought score, where higher values indicate greater injury, recovery was expressed as the percentage alleviation of injury relative to the stress level:

$$\text{Injury alleviation (\%)} = 100 \times [1 - (\text{Recovery} / \text{Stress})]$$

2.6 Data analysis

Values are presented as means ± standard error (SE) based on four subsamples per cultivar × treatment × sampling time; the subsamples were not independent experimental replicates. Changes during stress and recovery were expressed as percentage reduction and percentage recovery relative to the corresponding control and severe-stress values, respectively. Differences among treatment conditions are therefore interpreted as descriptive responses rather than statistically tested treatment effects.

Logistic growth curves were fitted separately for each cultivar × treatment combination using nonlinear least-squares regression with the *nls* function. Model fit was evaluated using the coefficient of determination (R^2) and root mean square error (RMSE), and parameter estimates were reported with their associated uncertainty estimates. Graphs were generated using the ggplot2 package [15].

3. Results and discussion

3.1 Tiller production, leaf rolling, and stress response

Figure 1 illustrates the descriptive responses of KW and RD6 rice cultivars to non-stress conditions and progressive PEG-induced osmotic stress over the experimental period, followed by recovery. Under non-stress conditions, TN increased progressively in both cultivars, with KW generally producing more tillers than RD6. Lower TN values were observed under progressive PEG-induced osmotic stress. At day 14 under 25% PEG, TN was 3.8 ± 0.5 in KW and 2.8 ± 1.7 in RD6, corresponding to reductions of approximately 73% and 65%, respectively, relative to their respective non-stress conditions. These observations show a pronounced decline in tiller production under severe osmotic stress. Similar reductions in tiller production under osmotic stress have

been reported in rice and have been associated with restricted cell expansion, impaired photosynthesis, and reduced assimilate availability under water-deficit conditions [16, 17]. During recovery, TN increased in both cultivars, reaching 4.3 ± 3.6 in KW and 5.8 ± 2.7 in RD6. Relative to the corresponding control values at recovery, these values represented 21% and 52%, respectively, indicating a greater descriptive recovery of tiller production in RD6 than in KW (Figure 1A).

LRS remained at the baseline level (score = 1) under non-stress conditions, whereas it increased with increasing PEG concentration and stress duration. At day 14 under 25% PEG, LRS reached 4.3 ± 0.3 in KW and 4.0 ± 0.6 in RD6, corresponding to stress increases of approximately 76% and 75%, respectively, relative to the corresponding non-stress baseline values (Figure 1B). At day 7, LRS was descriptively higher in RD6 (1.8 ± 0.8) than in KW (1.0 ± 0.0). Leaf rolling is an important drought-avoidance response in rice because it can reduce transpiration and help conserve water under dehydration conditions; however, severe leaf rolling may also restrict photosynthetic activity and plant growth [18]. During recovery, LRS decreased to 3.0 ± 1.0 in KW and 3.0 ± 0.0 in RD6, representing reductions of approximately 29% and 25%, respectively, relative to their corresponding severe-stress values. Thus, both cultivars showed a partial alleviation of leaf rolling following stress removal.

DS remained at zero under non-stress conditions but increased progressively with increasing PEG concentration and stress duration, indicating increasing visible stress symptoms. At day 7, DS was descriptively higher in RD6 (3.0 ± 1.7) than in KW (1.0 ± 0.0). Under 25% PEG at day 14, DS reached 7.8 ± 0.3 in KW and 6.8 ± 1.3 in RD6, corresponding to 86% and 75%, respectively, of the maximum score of 9 (Figure 1C). During recovery, DS decreased to 6.8 ± 1.7 in KW and 5.0 ± 1.4 in RD6, corresponding to reductions of approximately 13% and 26%, respectively, relative to the severe-stress values. The greater numerical reduction in DS in RD6 suggests a stronger descriptive alleviation of visible stress symptoms following stress removal. Similar differential recovery responses among rice genotypes following drought stress have been reported [19].

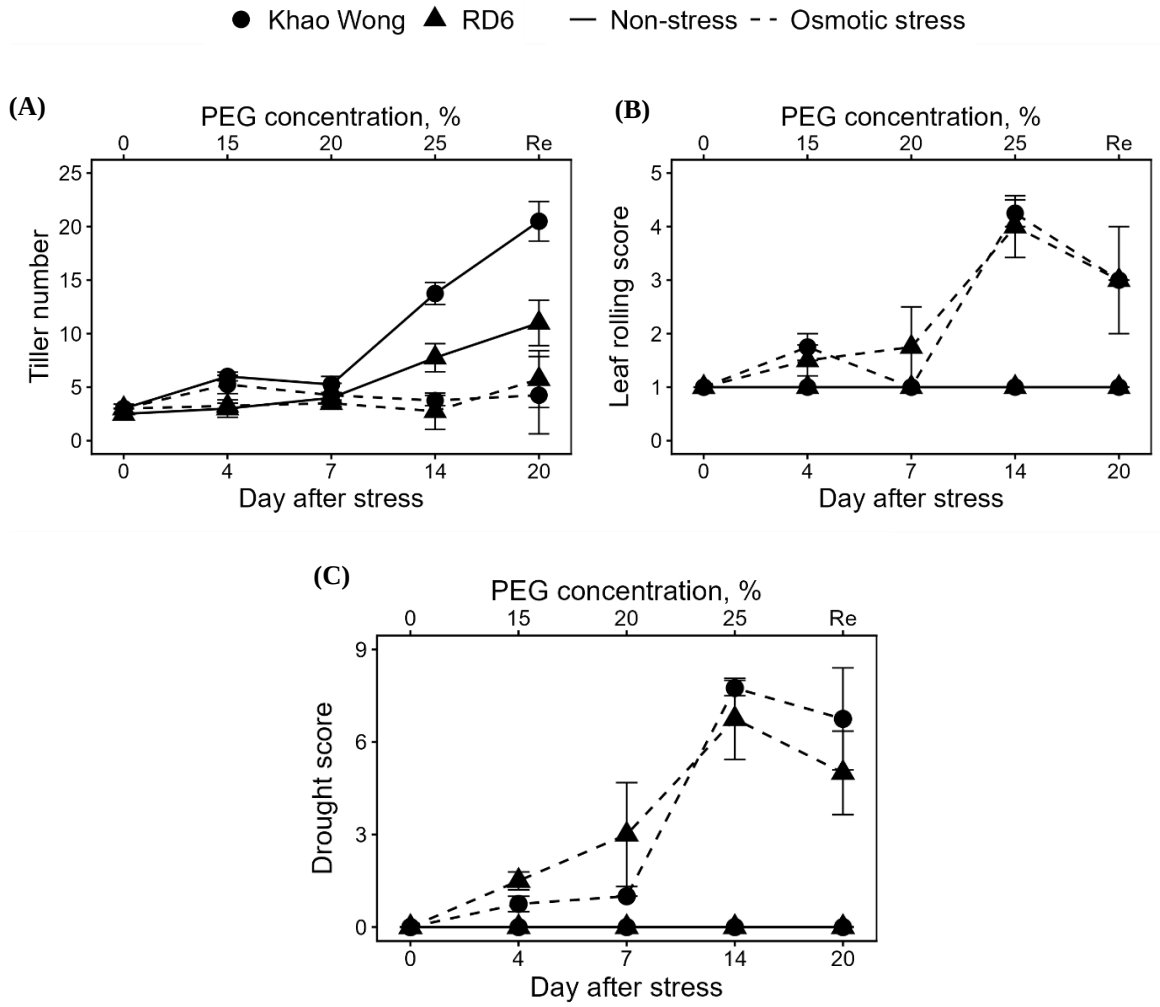


Figure 1 Changes in tiller number (A), leaf rolling score (B), and drought score (C) of Khao Wong and RD6 rice cultivars under progressive PEG-induced osmotic stress and recovery. Values are means ± SE. Re, recovery.

3.2 Biomass accumulation and allocation

Under non-stress conditions, shoot dry mass (S_Md) increased progressively over time in both cultivars, with KW generally showing higher values than RD6. Under progressive PEG-induced osmotic stress, S_Md accumulation was lower than under non-stress conditions, particularly at the later stages of stress. At 25% PEG, S_Md reached 0.84 ± 0.17 g plant^{-1} in KW and 0.96 ± 0.50 g plant^{-1} in RD6, compared with 4.18 ± 0.39 and 2.79 ± 0.37 g plant^{-1}, respectively, under the corresponding non-stress conditions. These values represented descriptive reductions of approximately 80% in KW and 65% in RD6. The larger numerical reduction observed in KW is consistent with greater sensitivity of shoot biomass accumulation under the progressive PEG treatment. However, because PEG concentration increased progressively with exposure time, the observed response reflects the combined effects of increasing osmotic stress intensity and stress duration rather than PEG concentration alone. Similar reductions in shoot biomass under water-deficit and salt stress have been reported, with combined stresses further intensifying growth inhibition and biomass loss [20]. During recovery, S_Md increased to 1.32 ± 1.15 g plant^{-1} in KW and 1.43 ± 0.41 g plant^{-1} in RD6, corresponding to approximately 15% and 25% of their respective non-stress control values at the recovery stage. Thus, shoot biomass remained substantially below the corresponding control levels, indicating incomplete recovery (Figure 2A).

Root dry mass (R_Md) showed a broadly similar temporal pattern. Under non-stress conditions, R_Md increased progressively, with KW generally maintaining higher values than RD6. Under progressive PEG-induced osmotic stress, root biomass accumulation was increasingly constrained at the later stages. At 25% PEG, R_Md reached 0.25 ± 0.05 g plant^{-1} in KW and 0.36 ± 0.18 g plant^{-1} in RD6, compared with 1.10 ± 0.10 and 0.66 ± 0.08 g plant^{-1}, respectively, under non-stress conditions. The corresponding reductions were approximately 78% in KW and 45% in RD6, indicating a larger descriptive reduction in root biomass accumulation in KW. Water deficit during the vegetative stage has similarly been reported to reduce root dry matter accumulation [21]. During recovery, R_Md increased to 0.47 ± 0.38 g plant^{-1} in KW and 0.50 ± 0.15 g plant^{-1} in RD6. These values corresponded to approximately 21% and 32%, respectively, of the corresponding non-stress control values, indicating that root biomass remained well below the control level after stress removal (Figure 2B).

The shoot dry-to-fresh mass ratio (S_Md/Mf) was relatively stable under non-stress conditions but increased progressively under PEG-induced osmotic stress. At 25% PEG, the ratio reached 29.52 ± 1.29 in KW and 34.56 ± 4.75 in RD6, compared with 15.18 ± 0.07 and 16.66 ± 0.13, respectively, under the corresponding non-stress conditions. These values represented increases of approximately 48% in KW and 52% in RD6. Because fresh mass reflects tissue water content to a large extent, the increase in S_Md/Mf indicates a greater proportion of dry matter relative to fresh mass and is consistent with reduced tissue hydration under progressive osmotic stress. The higher ratio observed in RD6 at 25% PEG suggests a greater shift in the balance between dry matter and fresh mass at the severe stress stage. During recovery, the ratio decreased to 14.58 ± 1.07 in KW and 17.16 ± 1.09 in RD6, approaching the corresponding non-stress values of 17.94 ± 0.07 and 19.29 ± 0.44, respectively. This decline indicates an improvement in the dry-to-fresh mass relationship following PEG removal (Figure 2C).

The root-to-shoot dry mass ratio (Md_R/S) remained relatively stable under the non-stress conditions but showed cultivar-dependent changes under progressive PEG-induced osmotic stress. At 25% PEG, Md_R/S increased to 0.29 ± 0.01 in KW and 0.45 ± 0.11 in RD6, compared with 0.26 ± 0.02 and 0.24 ± 0.02, respectively, under the corresponding non-stress conditions. These values represented increases of approximately 11% in KW and 47% in RD6. The greater increase in RD6 indicates a larger shift in the relative distribution of dry mass between roots and shoots, consistent with a proportionally greater reduction in shoot biomass relative to root biomass. Similar increases in root-to-shoot ratios under water-deficit conditions have been reported and may be associated with altered assimilate partitioning toward roots [22]. During recovery, Md_R/S decreased to 0.43 ± 0.08 in KW and 0.34 ± 0.04 in RD6. The ratio therefore remained above the corresponding non-stress values in both cultivars, particularly in KW, indicating that biomass allocation had not completely returned to the non-stress pattern (Figure 2D).

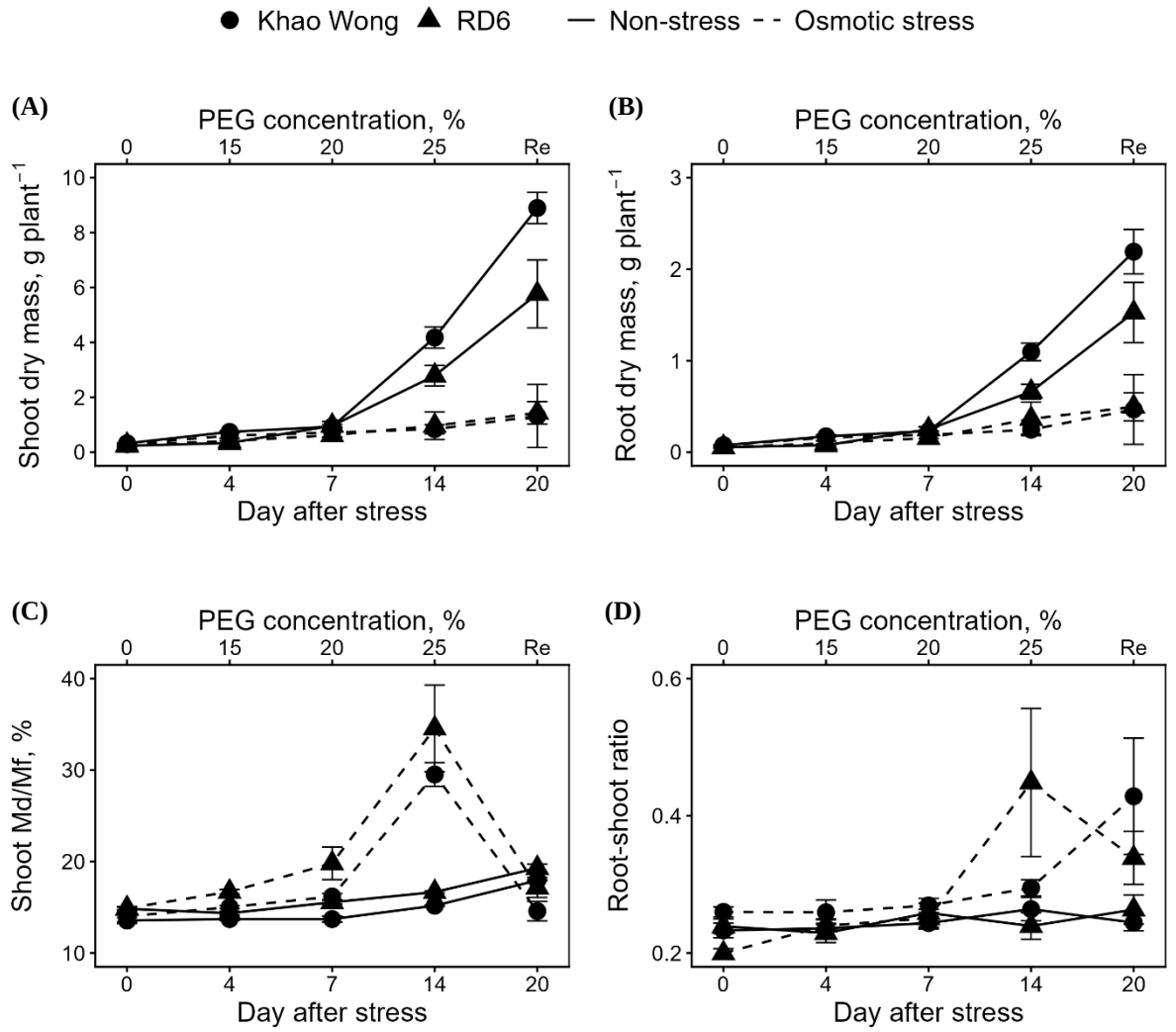


Figure 2 Shoot and root biomass and biomass allocation of Khao Wong and RD6 cultivars under progressive PEG-induced osmotic stress and recovery. A) Shoot dry mass (S_Md), B) root dry mass (R_Md), C) shoot dry mass-to-fresh mass ratio (S_Md/Mf), and D) root-to-shoot dry mass ratio (Md_R/S). Values are means ± SE. Re, recovery.

3.3 Growth dynamics and logistic model analysis

Crop models are valuable analytical tools for understanding crop growth and development, evaluating plant responses to environmental conditions, and predicting important crop management stages [23]. In the present study, total dry mass accumulation during the seedling stage was characterized over the 20-day experimental period using a logistic growth model to compare growth dynamics under non-stress and progressive PEG-induced osmotic stress. The logistic model adequately described total dry mass accumulation in both cultivars and treatments, as indicated by high coefficients of determination (R^2 = 0.996–0.999) and low RMSE values (0.017–0.138) (Table 1). Total dry mass accumulation followed a typical sigmoidal pattern under non-stress conditions, whereas biomass accumulation was markedly restricted under progressive PEG stress (Figure 3A). Similar applications of logistic models have been reported for characterizing crop growth responses to environmental stress [24].

Under non-stress conditions, total dry mass increased progressively in both cultivars, with KW consistently showing greater biomass accumulation than RD6. Differences between non-stress and progressive PEG-induced osmotic stress conditions became evident after approximately day 7, with stressed plants showing substantially slower biomass accumulation. The estimated maximum total dry mass (Md_m) was 17.8 g plant^{-1} for KW and 13.8 g plant^{-1} for RD6 under non-stress conditions. Under progressive PEG-induced osmotic stress, Md_m decreased to 1.09 and 1.95 g plant^{-1}, respectively, corresponding to reductions of 94% in KW and 86% in RD6 relative to the corresponding non-stress estimates (Table 1; Figure 3A). Model parameters (Md_0, Md_m, and α), together with their standard errors and goodness-of-fit statistics (R^2 and RMSE), are presented for each cultivar ×

treatment combination in Table 1. These results show that the magnitude of biomass accumulation was substantially lower under progressive PEG-induced osmotic stress in both cultivars.

The instantaneous growth rate (dMd/dt) derived from the logistic model showed a unimodal pattern under non-stress conditions, indicating a period of maximum biomass accumulation. Under non-stress conditions, the maximum predicted growth rates of KW and RD6 were 1.022 and 0.691 g plant^{-1} day^{-1}, occurring at approximately days 17.8 and 19.4, respectively (Table 1; Figure 3B). Under progressive PEG stress, the maximum predicted growth rates decreased markedly to 0.094 g plant^{-1} day^{-1} at approximately day 1.8 in KW and 0.085 g plant^{-1} day^{-1} at approximately day 9.6 in RD6. These results show that the magnitude of biomass accumulation was substantially lower under progressive PEG-induced osmotic stress in both cultivars.

The parameter α represents the logistic rate parameter governing the temporal pattern and steepness of biomass accumulation, rather than a directly measured absolute growth rate or the time required to reach maximum growth. The estimated α values were 0.229 and 0.201 day^{-1} for KW and RD6 under non-stress conditions, respectively, and 0.344 and 0.175 day^{-1} under progressive PEG stress. Because α interacts with the other logistic parameters, particularly Md_0 and Md_m, it should not be interpreted independently as an indicator of superior growth or osmotic stress tolerance. For example, although KW showed a higher α under progressive PEG stress, its predicted Md_m and maximum growth rate were substantially lower than those under non-stress conditions. Thus, the combined interpretation of α, Md_m, and dMd/dt provides a more appropriate description of growth dynamics.

Logistic modeling has also been applied to integrate multiple plant growth characteristics and characterize plant responses to environmental conditions [25]. In the present study, the logistic model effectively distinguished differences in total dry mass accumulation between KW and RD6 under progressive PEG-induced osmotic stress. The substantially lower predicted maximum biomass and maximum growth rates under stress were associated with lower predicted biomass accumulation in both cultivars, with KW showing a greater numerical reduction in predicted maximum biomass than RD6. These findings should be interpreted specifically as growth responses to progressive PEG-induced osmotic stress at the seedling stage. Because PEG concentration was increased sequentially over time, the responses at individual PEG concentrations reflect the combined effects of PEG concentration and cumulative stress duration and should not be interpreted as independent concentration effects.

Table 1 Estimated logistic growth parameters and goodness-of-fit statistics for total dry mass accumulation in KW and RD6 rice under non-stress and progressive PEG-induced osmotic stress.

Treatment	Cultivar	Md_0 (g plant^{-1})	Md_m (g plant^{-1})	α (day^{-1})	Max dMd/dt (g plant^{-1} day^{-1})	Day at max dMd/dt	R^2	RMSE
Non-stress	KW	0.294±0.08	17.80±2.86	0.229±0.03	1.022	17.8	0.999	0.138
	RD6	0.274±0.08	13.80±3.79	0.201±0.03	0.691	19.4	0.998	0.111
Osmotic Stress	KW	0.377±0.03	1.09±0.04	0.344±0.05	0.094	1.8	0.996	0.017
	RD6	0.307±0.04	1.95±0.49	0.175±0.04	0.085	9.6	0.997	0.022

Values are presented as parameter estimates ± SE. Maximum dMd/dt and the corresponding day represent the maximum predicted instantaneous growth rate within the experimental time range.

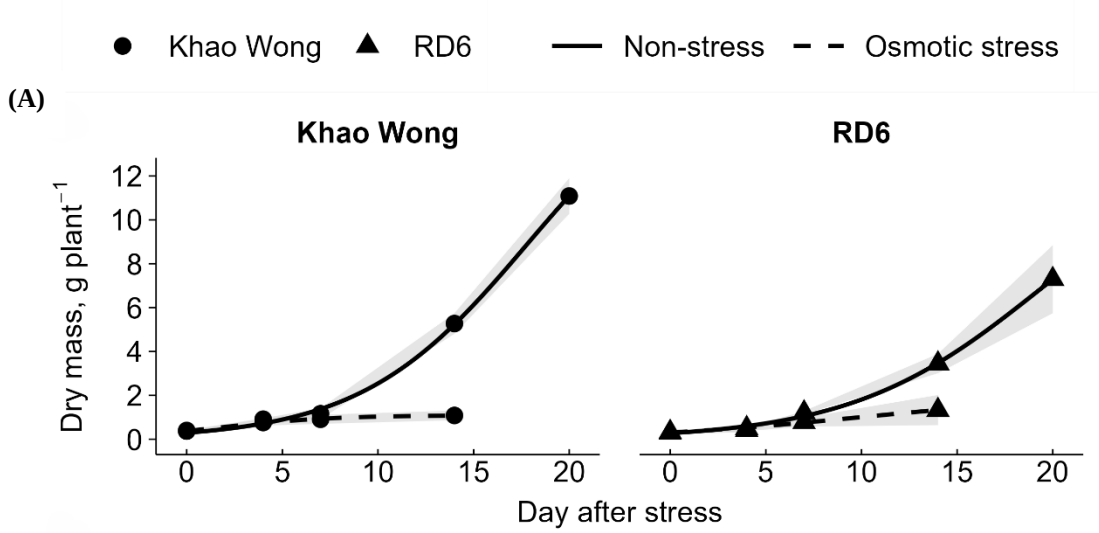


Figure 3 Total plant dry mass accumulation (A) and growth rate (B) of Khao Wong and RD6 cultivars under non-stress and PEG-induced osmotic stress. Total dry mass (g plant^{-1}) was described using a logistic growth model, and growth rate (dMd/dt; g plant^{-1} day^{-1}) was derived from the fitted model. Data for day 20 under PEG-induced osmotic stress were excluded because plants had entered the recovery phase. Symbols • and ▲ represent mean ± SE, lines — and -- denote model predictions.

(B)

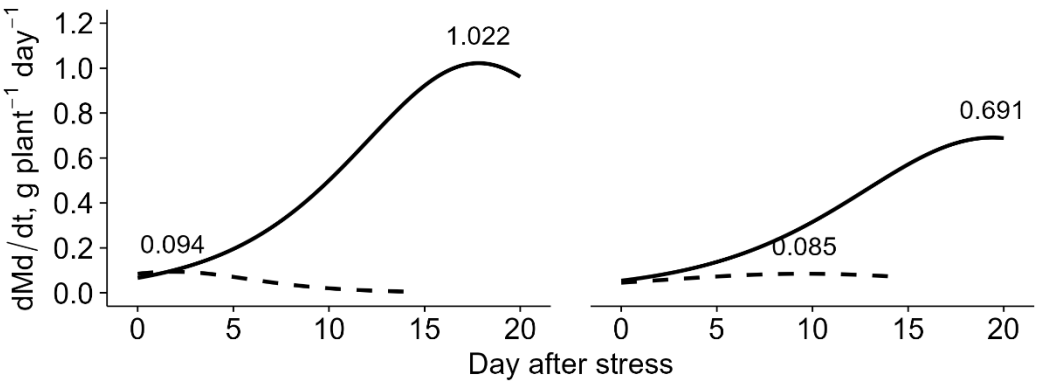


Figure 3 Total plant dry mass accumulation (A) and growth rate (B) of Khao Wong and RD6 cultivars under non-stress and PEG-induced osmotic stress. Total dry mass (g plant^{-1}) was described using a logistic growth model, and growth rate (dMd/dt; g plant^{-1} day^{-1}) was derived from the fitted model. Data for day 20 under PEG-induced osmotic stress were excluded because plants had entered the recovery phase. Symbols • and ▲ represent mean ± SE, lines — and -- denote model predictions. (Conf.)

3.4 Relative water content and cell membrane stability

Under non-stress conditions, RWC remained relatively high and stable (85–97%) in both cultivars across the sampling period (Figure 4A). Under progressive PEG-induced osmotic stress, RWC declined with increasing PEG concentration, with the lowest values observed at 25% PEG (day 14). At this stage, RWC decreased to 24.18 ± 9.7% in KW and 40.50 ± 6.3% in RD6, corresponding to numerical reductions of 73% and 55%, respectively, relative to their corresponding non-stress controls. Thus, KW showed a greater numerical decline in RWC than RD6 under severe PEG-induced osmotic stress. Following PEG removal, RWC increased substantially in both cultivars, reaching 91.22 ± 1.1% in KW and 100.00 ± 0.0% in RD6, compared with 95.10 ± 1.2% and 96.69 ± 0.6% in their respective controls. These values indicate a numerical improvement in plant water status following stress removal, with RWC approaching or reaching the corresponding control levels.

The RWC response observed in the present study is consistent with previous reports of declining RWC with increasing PEG concentration. Chen et al. (2020) reported reduced RWC under 20% and 25% PEG-induced osmotic stress [26], while Sandhu et al. (2012) observed a progressive decline in RWC with increasing PEG concentration [27].

Cell membrane stability (CMS) remained relatively stable under non-stress conditions, ranging from 79 to 91% in both cultivars (Figure 4B). Under progressive PEG-induced osmotic stress, CMS declined numerically at higher PEG concentrations, particularly between days 7 and 14. At 25% PEG (day 14), CMS decreased to 24.82 ± 4.6% in KW and 33.99 ± 11.7% in RD6, corresponding to numerical reductions of 73% and 61%, respectively, relative to the corresponding controls. These changes indicate greater membrane injury under severe PEG-induced osmotic stress, with KW showing a greater numerical decline than RD6. Following PEG removal, CMS increased markedly to 86.28 ± 2.1% in KW and 83.62 ± 2.2% in RD6, compared with 86.35 ± 2.3% and 85.64 ± 1.6% in the respective controls. Thus, CMS numerically approached the non-stress levels during recovery, indicating improved membrane stability following stress removal.

Alamgir (2023) reported greater membrane stability in rice varieties characterized as drought-tolerant [28]. In the present study, however, the observed CMS differences are interpreted specifically as responses to PEG-induced osmotic stress rather than as evidence of drought tolerance under soil or field conditions.

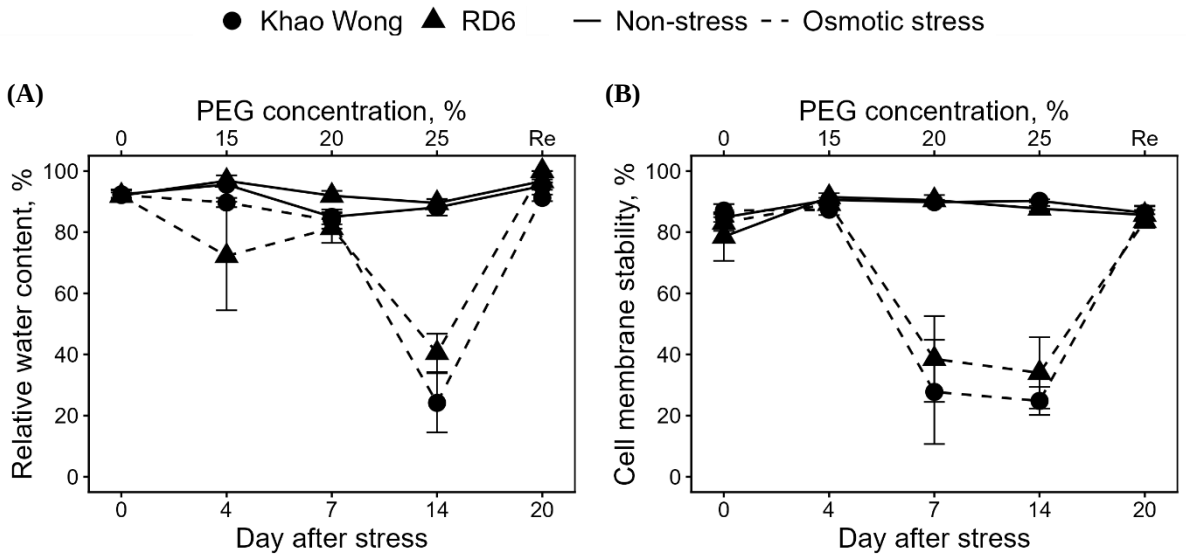


Figure 4 Water status and cell membrane stability of Khao Wong and RD6 cultivars under progressive PEG-induced osmotic stress and recovery. A) Relative water content and B) cell membrane stability. Values are means ± SE. Re, recovery.

3.5 Chlorophyll responses to progressive PEG-induced osmotic stress

Chl_a (Figure 5A) remained relatively stable under non-stress conditions, with values generally around 0.3 g m^{-2} in both cultivars. Under progressive PEG-induced osmotic stress, Chl_a showed a variable response, with the lowest values observed at 25% PEG (day 14). At this stage, Chl_a decreased to 0.17 ± 0.03 g m^{-2} in KW and 0.09 ± 0.05 g m^{-2} in RD6, corresponding to numerical reductions of 40% and 66%, respectively, relative to the corresponding non-stress values. Thus, RD6 showed a greater numerical decline in Chl_a than KW under severe PEG-induced osmotic stress. Following PEG removal, Chl_a increased in both cultivars, reaching 0.32 ± 0.06 g m^{-2} in KW and 0.33 ± 0.05 g m^{-2} in RD6, corresponding to approximately 98% and 99% of their respective non-stress values. These changes indicate a substantial numerical improvement in Chl_a following stress removal.

Chl_b (Figure 5B) showed a less pronounced and more variable response to progressive PEG-induced osmotic stress. At 25% PEG (day 14), Chl_b decreased to 0.07 ± 0.01 g m^{-2} in KW and 0.07 ± 0.03 g m^{-2} in RD6, corresponding to numerical reductions of 12% and 45%, respectively, relative to the corresponding non-stress values. The greater numerical reduction in RD6 indicated a stronger decline in Chl_b under severe osmotic stress. Following PEG removal, Chl_b increased in both cultivars, reaching 0.16 ± 0.05 g m^{-2} in KW and 0.09 ± 0.03 g m^{-2} in RD6. These values corresponded to approximately 89% and 63% of the respective non-stress levels, indicating partial numerical recovery of Chl_b following stress removal.

Chl_{total} (Figure 5C) remained relatively stable under non-stress conditions throughout the experimental period. Under progressive PEG-induced osmotic stress, Chl_{total} showed a transient increase at 15% PEG (day 4), followed by a decline at higher PEG concentrations, reaching the lowest values at 25% PEG (day 14). At day 14, Chl_{total} decreased to 0.24 ± 0.04 g m^{-2} in KW and 0.23 ± 0.05 g m^{-2} in RD6, corresponding to numerical reductions of 34% and 42%, respectively, relative to the corresponding non-stress values. Thus, RD6 showed a greater numerical reduction in total chlorophyll at the severe stage of progressive PEG-induced osmotic stress. Following PEG removal, Chl_{total} increased to 0.47 ± 0.01 g m^{-2} in KW and 0.43 ± 0.03 g m^{-2} in RD6, corresponding to approximately 95% and 93% of the respective non-stress values. These responses indicate substantial numerical improvement in total chlorophyll following stress removal.

The $Chl_{a/b}$ ratio (Figure 5D) varied across sampling stages and cultivars. Under progressive PEG-induced osmotic stress, the ratio increased at intermediate stress stages, particularly around day 7, reflecting changes in the relative proportions of Chl_a and Chl_b. At 25% PEG (day 14), the $Chl_{a/b}$ ratio declined to 2.55 ± 0.47 in KW and 1.43 ± 0.56 in RD6, compared with 3.67 ± 0.21 and 2.93 ± 1.00, respectively, under non-stress conditions. Following PEG removal, the ratio increased to 2.10 ± 0.25 in KW and 2.79 ± 0.01 in RD6. These values were approximately 108% and 118% of the corresponding non-stress values, respectively, indicating a numerical shift in chlorophyll composition following stress removal.

Alterations in photosynthetic pigments under PEG-induced osmotic stress have also been reported. Saha et al. (2020) observed reductions in Chl_a, Chl_b, total chlorophyll, carotenoids, and the $Chl_{a/b}$ ratio under drought stress [29], while Yang et al. (2024) reported reductions of 11–32% in Chl_a and Chl_b under stress conditions [30].

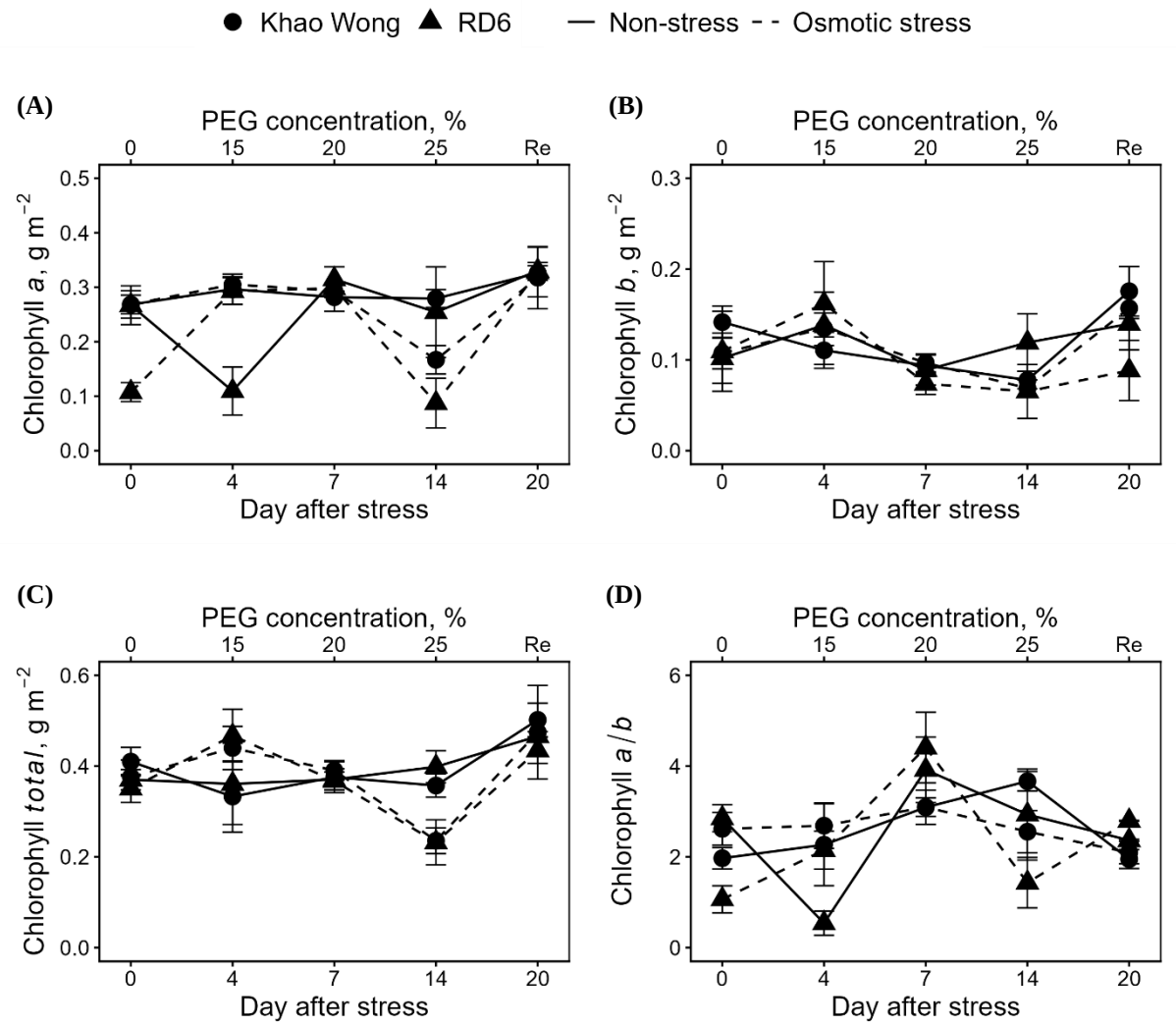


Figure 5 Photosynthetic pigment responses of Khao Wong and RD6 cultivars under progressive PEG-induced osmotic stress and recovery. A) Chlorophyll *a* (Chl_a), B) chlorophyll *b* (Chl_b), C) total chlorophyll (Chl_{total}), and D) chlorophyll *a/b* ratio ($Chl_{a/b}$). Values are means ± SE. Re, recovery.

4. Conclusion

Under the experimental conditions used here, progressive PEG-induced osmotic stress was associated with numerical reductions in tiller production, shoot and root biomass, RWC, CMS, and several chlorophyll traits, together with increases in LRS and DS. KW produced greater biomass under non-stress conditions but generally exhibited larger numerical reductions in biomass and water-related traits under progressive osmotic stress, whereas RD6 maintained relatively higher biomass, RWC, and CMS under the more severe stress stages. Logistic growth analysis showed substantially lower predicted maximum biomass (Md_m) and instantaneous growth rate (dMd/dt) under progressive PEG stress, with a greater numerical reduction in Md_m in KW.

Following PEG removal, several traits increased in both cultivars, but recovery varied among traits and cultivars and did not consistently restore values to non-stress levels. In particular, increases in chlorophyll content during recovery should be interpreted as changes in pigment content rather than direct evidence of complete restoration of photosynthetic function. Overall, KW and RD6 exhibited distinct physiological and agronomic trait responses to progressive PEG-induced osmotic stress under hydroponic conditions at the seedling stage. Further soil- and field-based studies are required to determine whether these responses are associated with drought tolerance or adaptation under rainfed conditions.

5. Acknowledgements

We gratefully acknowledge the Faculty of Agricultural Technology, Kalasin University, for providing the equipment and facilities necessary for this research, including greenhouse and laboratory facilities. We would like

to thank Jonathan Benoit Virgile Elisabeth Wary, Faculty of Liberal Arts, Kalasin University, for English proofreading.

6. Author Contributions

PK: Conceptualization, Formal analysis, Investigation, Project administration, Visualization, Writing – review & editing; PB, TB and NK: Investigation; UK and KP: Resources.

7. References

[1] Prabnakorn S, Maskey S, Suryadi F, de Fraiture C. Rice yield in response to climate trends and drought index in the Mun River Basin, Thailand. Sci Total Environ. 2018;621:108-119.
[2] Pairintra S, Wonprasaid S, Machikowa T. Responses of physiological traits, growth and yield of rice to drought stress. Agric Nat Resour. 2023;57(4):587-596.
[3] Urmi TA, Islam MM, Zumur KN, Abedin MA, Haque MM, Siddiqui MH, et al. Combined effect of salicylic acid and proline mitigates drought stress in rice (*Oryza sativa* L.) through the modulation of physiological attributes and antioxidant enzymes. Antioxidants. 2023;12(7):1438.
[4] Kumar A, Dixit S, Ram T, Yadaw R, Mishra K, Mandal N. Breeding high-yielding drought-tolerant rice: genetic variations and conventional and molecular approaches. J Exp Bot. 2014;65(21):6265-6278.
[5] Zheng X, Peng Y, Qiao J, Henry R, Qian Q. Wild rice: unlocking the future of rice breeding. Plant Biotechnol J. 2024;22(11):3218-3226.
[6] DIP. Geographical Indication: Department of Intellectual Property [Internet]. 2009 [cited 2026 May 8]. Available from https://www.ipthailand.go.th/th/home.html.
[7] Balansag GVA, Anud E, Balansag GPA, Anud K, Balansag GNA. The effect of ab mix nutrient solution on the height, number of leaves and fresh weight of lettuce (*Lactuca sativa* L.) in hydroponics cultivation system. Int J Appl Sci Res 2023;6(10.56293).
[8] O'toole J, Cruz R, Singh T. Leaf rolling and transpiration. Plant Sci Lett. 1979;16(1):111-114.
[9] De Datta S, Malabuyoc J, Aragon E. A field screening technique for evaluating rice germplasm for drought tolerance during the vegetative stage. Field Crops Res. 1988;19(2):123-134.
[10] Thornley JH, Johnson IR. Plant and crop modelling: Clarendon Oxford; 1990.
[11] Hunt R. Plant growth curves. The functional approach to plant growth analysis. 1982.
[12] Moran R. Formulae for determination of chlorophyllous pigments extracted with N, N-dimethylformamide. Plant Physiol. 1982;69(6):1376-1381.
[13] Alam MS, Tester M, Fiene G, Mousa MAA. Early growth stage characterization and the biochemical responses for salinity stress in tomato. Plants. 2021;10(4):712.
[14] Yin J, Bauerle TL. A global analysis of plant recovery performance from water stress. Oikos. 2017;126(10):1377-1388.
[15] R Core Team. R: a language and environment for statistical computing. Foundation for Statistical Computing. Vienna, Austria. 2023.
[16] Reddy INBL, Kim B-K, Yoon I-S, Kim K-H, Kwon T-R. Salt tolerance in rice: focus on mechanisms and approaches. Rice Sci. 2017;24(3):123-144.
[17] Kalaitzidis A, Kadoglidou K, Mylonas I, Ghoghoberidze S, Ninou E, Katsantonis D. Investigating the impact of tillering on yield and yield-related traits in European rice cultivars. Agriculture. 2025;15(6):616.
[18] Jarin AS, Islam MM, Rahat A, Ahmed S, Ghosh P, Murata Y. Drought stress tolerance in rice: physiological and biochemical insights. Int J Plant Biol. 2024;15(3):692-718.
[19] Swapna S, Shylaraj KS. Screening for osmotic stress responses in rice varieties under drought condition. Rice Sci. 2017;24(5):253-263.
[20] Huanhe W, Xiaoyu G, Xiang Z, Wang Z, Xubin Z, Yinglong C, et al. Grain yield, biomass accumulation, and leaf photosynthetic characteristics of rice under combined salinity-drought stress. Rice Sci. 2024;31(1):118-128.
[21] Adzigbe J, Frimpong F, Danquah A, Danquah EY, Asante IK, Abebrese SO, et al. The responses and adaptations of rice (*Oryza sativa* L.) to drought stress: a review. Clim Smart Agric. 2025:100080.
[22] Xu W, Cui K, Xu A, Nie L, Huang J, Peng S. Drought stress condition increases root to shoot ratio via alteration of carbohydrate partitioning and enzymatic activity in rice seedlings. Acta Physiol Plant. 2015;37(2):9.
[23] Hsieh C-Y, Chen H, Wu Y-C, Teng C-Y, Li C-H. Using critical points of logistic model to describe the growth of rice plant height in Taiwan. Sci Rep. 2026;16(1):10081.

[24] Wang N, Liu Q, Ming B, Shang W, Zhao X, Wang X, et al. Impacts of heat stress around flowering on growth and development dynamic of maize (*Zea mays* L.) ear and yield formation. Plants. 2022;11(24):3515.

[25] Kharraz N, Szabó I. Extending Logistic Growth for Smart Agriculture: A Four-Dimensional Model Integrating Photosynthesis and Resource Efficiency. Smart Agric Technol. 2025:101240.

[26] Chen Z, Xu W, Nie J, Khan A, Cao C, Li P. Drought stress intensity, duration and its resistance impact on rice (*Oryza sativa* L.) seedling. Appl Ecol Environ Res. 2020;18(1):469.

[27] Sandhu N, Jain S, Battan K, Jain R. Aerobic rice genotypes displayed greater adaptation to water-limited cultivation and tolerance to polyethyleneglycol-6000 induced stress. Physiol Mol Biol Plants. 2012;18(1):33-43.

[28] Alamgir A. Cell membrane injury, stability and atpase actibity and their relevance to seed germination, seedling growth tolerance indices of rice under abiotic stresses. Bangladesh J Bot. 2023;52(3):889-896.

[29] Saha S, Begum HH, Nasrin S, Samad R. Effects of drought stress on pigment and protein contents and antioxidant enzyme activities in five varieties of rice (*Oryza sativa* L.). Bangladesh J Bot. 2020;49(4):997-1002.

[30] Yang X, Wang X, Li Y, Yang L, Hu L, Han Y, et al. Effects of drought stress at the booting stage on leaf physiological characteristics and yield of rice. Plants. 2024;13(24):3464.